


Oncogenic Long Noncoding RNA DARS-AS1 in Childhood Acute Myeloid Leukemia by Binding to microRNA-425

Technology in Cancer Research & Treatment
 Volume 19: 1-12
 © The Author(s) 2020
 Article reuse guidelines:
sagepub.com/journals-permissions
 DOI: 10.1177/1533033820965580
journals.sagepub.com/home/tct


Binghua Dou, MM¹, Zhu Jiang, MM², Xiaoguang Chen, MM¹, Chunmei Wang, MD¹, Jing Wu, MD¹, Jindou An, MB¹, and Guangyao Sheng, MM¹ 

Abstract

Objective: Acute myeloid leukemia (AML) represents a hematological cancer. The aim of the investigation was to probe the regulatory relevance of long non-coding RNA (lncRNA) aspartyl-tRNA synthetase anti-sense 1 (DARS-AS1)/microRNA-425 (miR-425)/transforming growth factor-beta 1 (TGFB1) to the development of AML. **Methods:** The DARS-AS1 expression in bone marrow tissues was first analyzed in healthy subjects and AML patients. Subsequently, AML cell lines with DARS-AS1 knockdown were constructed, followed by cell proliferation and apoptosis assays. Afterward, downstream miRNA of DARS-AS1 and target mRNA of the miRNA were analyzed by bioinformatics, and their binding relationships were verified. Functional rescue experiments were then implemented. Finally, activation of the Smad2/3 signaling in MV4-11 and BF-24 cells were detected by western blot. **Results:** DARS-AS1 was overexpressed in bone marrow tissues of AML patients and cells, and DARS-AS1 knockdown suppressed the proliferation of AML cells and induced apoptosis. DARS-AS1 bound to and negatively correlated with miR-425. Further results suggested that TGFB1 might be a target gene of miR-425 and could promote Smad2/3 phosphorylation and nuclear translocation. Finally, DARS-AS1 depletion could diminish the tumor volume *in vivo*. **Conclusion:** All in all, we highlighted here that DARS-AS1 enhanced the expression of TGFB1 through binding to miR-425 to modulate AML progression via the Smad2/3 pathway, which might perform as a therapeutic target for AML.

Keywords

acute myeloid leukemia, DARS-AS1, microRNA-425, TGFB1, Smad2/3 signaling

Abbreviations

AML, acute myeloid leukemia; ANOVA, analysis of variance; CCK-8, cell counting kit-8; DARS-AS1, aspartyl-tRNA synthetase anti-sense 1; EdU, 5-Ethynyl-2'-deoxyuridine; FISH, fluorescence in situ hybridization; lncRNA, long non-coding RNA; miR-425, microRNA-425; MT, mutant-type; OD, optical density; PI, propidium iodide; RT-qPCR, reverse transcription-quantitative polymerase chain reaction; SD, standard deviation; shRNA, short hairpin RNA; TGFB1, transforming growth factor-beta 1; WT, wild-type; 3'UTR, 3'untranslated region

Received: July 22, 2020; Revised: September 9, 2020; Accepted: September 22, 2020.

Introduction

Acute myeloid leukemia (AML) remains a relatively rare malignancy with a median age of diagnoses in the late 60 s, and the incidence is 2 to 3 per 100,000 for younger patients.¹ The outcome in older patients that are unable to be subjected to intensive chemotherapy remains unsatisfactory, with a median survival of 5 to 10 months.² While the outcome for children with AML has improved tremendously over the past 3 decades,

¹ Department of Paediatrics, The First Affiliated Hospital of Zhengzhou University, Zhengzhou, Henan, People's Republic of China

² Department of Ultrasound, The Third Affiliated Hospital of Zhengzhou University, Zhengzhou, Henan, People's Republic of China

Corresponding Author:

Guangyao Sheng, Department of Paediatrics, The First Affiliated Hospital of Zhengzhou University, No. 1, Jianshe East Road, Erqi District, Zhengzhou 450000, Henan, People's Republic of China.
 Email: SGuangYao4251@163.com



Table 1. Primer Sequences.

Targets	Forward (5'-3')	Reverse (5'-3')
DARS-AS1	AGCCAAGGACTGGTCTCTTTT	CTGTACTGGTGGGAAGAG
TGFB1	TACCTGAACCCGTGTTGCTCTC	GTTGCTGAGGTATCGCCAGGAA
GAPDH	GCAAGTTCAACGGCACAG	GCCAGTAGACTCCACGACA
miR-425	ATGACACGATCACTCCC	GAACATGTCTGCGTATCTC
U6	CTCGCTTCGGCAGCACACA	AACGCTTCACGAATTTGCGT

Note: DARS-AS1, aspartyl-tRNA synthetase anti-sense 1; TGFB1, transforming growth factor-beta 1; GAPDH, glyceraldehyde-3-phosphate dehydrogenase; miR-425, microRNA-425.

with complete remission and overall survival rate over 90% and 60%, respectively.³ Non-coding RNA transcripts that could not codify for proteins but play significant parts in the diagnosis, prognosis and therapeutic approaches of various cancers, including myeloid malignancies.⁴

Defined as transcripts of ~200 nucleotides without coding potency, long noncoding RNAs (lncRNAs) have the potency to engage in multiple cellular processes by modulating the different steps of gene expression, thus serving as promising biomarkers in many malignancies, including AML.⁵ Among them, aspartyl-tRNA synthetase anti-sense 1 (DARS-AS1), located in 2q21.3, is a new lncRNA discovered recently that has been identified as an onco-lncRNA in ovarian cancer and non-small cell lung cancer.^{6,7} As a consequence, we postulated that DARS-AS1 exerted a similar function in AML as well. Previously, another lncRNA colon cancer-associated transcript-1 has been underscored in AML by upregulating c-Myc expression through its competing endogenous RNA activity on microRNA (miR)-155.⁸ Also, DARS-AS1 positively regulated DARS expression via sponging miR-194-5p, thus contributing to malignancy in clear cell renal cell carcinoma.⁹ This kind of mechanism is established when endogenous RNA transcripts share mutual miRNA response elements to mediate expression of each other by competing for the same miRNA.¹⁰ In the current study, a bioinformatics tool RNA22 (<http://cm.jefferson.edu/rna22/>) predicted a possible binding relationship between miR-425 and DARS-AS1. miR-425 was observed to be poorly expressed in melanoma tissues and cells, and miR-425 mimic repressed melanoma cell proliferation and metastasis.¹¹ Moreover, another lncRNA small nucleolar RNA host gene 7 illustrated a tumor-supporting role in hepatic carcinoma cells through the Wnt/ β -catenin pathway as a miR-425 sponge.¹² However, its specific function in AML remains largely unclear. It was predicted by Targetscan (<http://www.targetscan.org/>) in our study that miR-425 can target transforming growth factor-beta 1 (TGFB1), the gene encoding TGF- β 1. TGF- β mainly plays as a driver in tumor progression and metastasis by augmenting tumor cell invasion, migration as well as chemoresistance at the advanced stage.¹³ Therefore, the present investigation was designed to probe the role of DARS-AS1 in the regulation of TGFB1 expression during AML progression by competitively binding to miR-425.

Materials and Methods

Clinical Samples

From July 2013 to October 2014, 59 AML patients (1-16 years, mean age 5.83 ± 3.61) and 34 gender- and age-matched healthy donors (0-14 years, mean age 6.4 ± 2.43 years) were enrolled at the First Affiliated Hospital of Zhengzhou University. Patients had Blasts of all nucleate cells $\geq 20\%$. All subjects underwent bone marrow aspiration and biopsy examination. The tissue samples were instantly frozen in an ultra-low temperature refrigerator at -80°C for temporary storage. The study was authorized by the Ethics Committee of the First Affiliated Hospital of Zhengzhou University (approval no. 201304011) with the permission of all participants and their guardians by providing informed consent.

RT-qPCR

Total RNA was isolated from bone marrow cells using TRIzol reagents (Invitrogen Inc., Carlsbad, CA, USA) and transcribed into cDNA using a PrimeScript RT kit (Takara Holdings Inc., Kyoto, Japan) with a gDNA eraser (Perfect Real-time, Takara). Real-time PCR was performed using SYBR Premix Ex Taq (TliRNase H Plus, Takara) following the manufacturer's instructions. Primer sequence details are presented in Table 1.

Cell Culture and Treatment

The human bone marrow stromal cells HS-5 were purchased from ATCC (Manassas, VA, USA) and AML cell lines (BF-24, MV4-11, U937 and HL-60) from China Center for Type Culture Collection (Wuhan, Hubei, China), respectively. All cells were grown in RPMI-1640 (Gibco) containing 10% FBS and 1% penicillin-streptomycin (Transgen, Beijing, China) at 37°C with 5% CO_2 .

MV4-11 and BF-24 cells were delivered with vectors or oligonucleotides according to the protocols of Lipofectamine 3000 (Invitrogen). Short hairpin RNA (shRNA) targeting DARS-AS1 (shDARS-AS1), Scramble (shScr), miR-425 inhibitor and inhibitor NC (Mock) were generated by GenePharma (Shanghai, China).

Colony Formation Assay

A total of 2×10^3 cells was cultured into 6-well plates containing the medium for 2 weeks. The colonies were fixed with 4% paraformaldehyde and then stained with GIMSA staining solution for 20 min. The number of colonies including ≥ 50 cells was counted under a microscope.

5-Ethynyl-2'-Deoxyuridine (EdU) Labelling

Cell proliferation was evaluated using Cell-Light™ EdU Apollo®567 In Vitro Imaging Kits (Guangzhou RiboBio, Guangzhou, Guangdong, China). Transfected cells were treated with 50 μ M EdU for a period of 1 h, fixed with formaldehyde at room temperature for 30 min and neutralized with formaldehyde by glycine for 5 min. Cells were then stained with Apollo staining solution at room temperature for 30 min, permeated by 0.5% Triton X-100 for 10 min and observed under a fluorescence microscope.

Cell Counting Kit-8 (CCK-8) Assay

CCK-8 (Bestbio, Shanghai, China) was used to measure cell proliferation capacity. Treated cells were plated in 96-well plates with 5000 cells each well and then cultured overnight. Subsequently, the optical density (OD) value was measured with the help of a microplate reader (Thermo Fisher Scientific Inc., Waltham, MA, USA) at 450 nm. The number of viable cells was tested every 24 h for 3 days.

Caspase-3 Activity Determination

Caspase-3 activity was used to measure apoptosis using Caspase-3 activity kits (Solarbio, Beijing, China). Total protein of the transfected MV4-11 and BF-24 cells was harvested and added to a 96-well plate containing assay buffer and caspase-3 substrate for a 4-h incubation. The determination of caspase-3 activity was performed at 405 nm by a microplate reader.

Flow Cytometry

The Annexin V-propidium iodide (PI) Kit (Nanjing Keygen, Nanjing, Jiangsu, China) was applied following the manufacturer's guidelines. Apoptotic cells were analyzed by a FACS Calibur using a CellQuest software (BD, San Jose, CA, USA).

Animal Experiments

A total of 20 six-week-old male NOD/SCID mice were purchased from the Nanjing Animal Research Center of Nanjing University (Nanjing, Jiangsu, China). All mice were allowed to acclimatize for 1 week in the animal facility under the specific-pathogen-free environment before any intervention was initiated. Mice were randomly categorized into 4 groups and injected subcutaneously with MV4-11 and BF-24 cells (1×10^6) stably transfected with shDARS-AS1 or empty vectors.

After 35 days, mice were euthanized by an intraperitoneal injection of excessive pentobarbital sodium with euthanasia confirmed successful by the absence of a heartbeat and a blinking reflex and the lack of spontaneous breathing. The tumor was removed for weighing.

Immunohistochemistry

Briefly, sections from paraffin-embedded xenograft tumors were treated with primary antibody against Ki-67 (ab15580, 1:500; Abcam, Cambridge, UK). Protein expression was evaluated using a Super Sensitive Link-Label IHC detection system (BioGenex company, Fremont, CA, USA).

FISH

FISH probes designed specifically for DARS-AS1 were commercially available from Ribobio and used on the basis of the guidelines. 4',6-diamidino-2-phenylindole (DAPI) solution was added for nuclear staining. Images were captured under a microscope to determine subcellular localization of DARS-AS1 in MV4-11 and BF-24 cells.

Nuclear/Cytoplasmic Fractionation

Nuclear/cytoplasmic fractionation was implemented using PARIS™ kits (Invitrogen) to detect the subcellular localization of DARS-AS1 in MV4-11 and BF-24 cells according to instructions of the manufacturer. The distribution of RNA in the nucleus and cytoplasm was assessed by RT-qPCR.

RNA Pull-Down Assays

Briefly, cell lysates were treated with biotinylated RNA containing Bio-miR-425-WT, Bio-miR-425-MT and Bio-negative control (NC). Next, M-280 streptavidin magnetic beads (Sigma-Aldrich Chemical Company, St Louis, MO, USA) were added for co-culture for 48 h. The relative enrichment of RNAs pulled-down in each group were determined by RT-qPCR.

Luciferase Reporter Assay

A total of 10^6 HEK293 T cells were cultured in 6-well plates and grown to 90% confluence before cell transfection. HEK293 T cells were delivered with pGL4 vector (Biofeng) recombined with DARS-AS1 WT and DARS-AS1 MT or TGFB1 WT and TGFB1 MT and miR-425 or mimic NC, respectively with lipofectamine 3000 (Invitrogen). After 48 h, the dual-luciferase reporter system (Thermo Fisher Scientific) was used for luciferase activity determination with Renilla luciferase activity for normalization.

Immunofluorescence

The cells were plated in a 12-well culture plate and then treated with phosphate buffered saline containing 0.5% Triton X-100

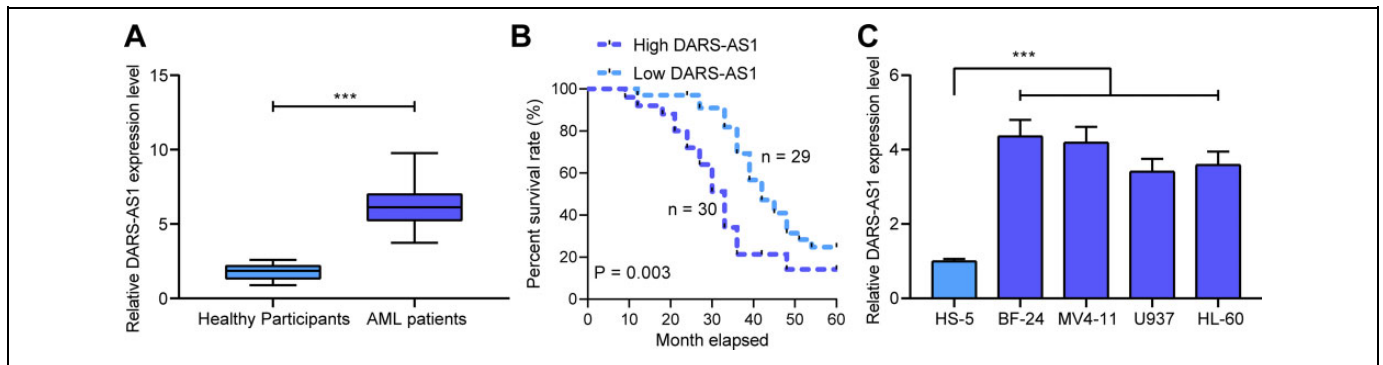


Figure 1. DARS-AS1 is significantly higher in AML patients and cell lines and is linked to unsatisfactory prognosis. A, RT-qPCR detection of DARS-AS1 expression in bone marrow from 34 healthy subjects and 59 AML patients; B, Kaplan-Meier analysis of DARS-AS1 and 5-year survival rate; C, RT-qPCR expression of DARS-AS1 in 4 AML cell lines and HS-5 cells. Data were represented as mean \pm SD of 3 individual experiments. Data between 2 groups was analyzed using paired *t*-test (panel A), and 1-way ANOVA followed by Tukey's post hoc test was utilized for data analysis among multiple groups (panel C). *** $p < 0.001$.

and 4% formaldehyde for 10 min. Subsequently, the cells were mixed with 5% bovine serum albumin for 30 min and incubated with Smad2/3 (ab76055, 1:500; Abcam) and secondary antibody (ab205719, 1:2000; Abcam). Samples treated with DAPI solution were analyzed under the microscope.

Western Blot

MV4-11 and BF-24 cells were lysed in lysis buffer containing 50 mM Tris-HCl (pH = 7.4), 150 mM NaCl, 1% Triton X-100, 0.1% sodium dodecyl sulfate, 1 mM ethylenediaminetetraacetic acid, 1 mM Na₃VO₄, 1 mM NaF and 1 \times proteinase inhibitor cocktail on ice and then centrifuged at 14,000 \times g for 20 min. The supernatant was collected, and the protein concentration was quantified using the RC DC protein assay kit (Bio-Rad, Hercules, CA, USA). The protein samples were separated by 4-12% NuPAGE Bis-Tris gel (Novex, Carlsbad, CA, USA) and transferred to the Hybond ECL membrane. Antibodies used included TGFB1 (1:2000, #GTX45121, GeneTex, Inc., Alton Pkwy Irvine, CA, USA), phosSmad2 (1:1000, #18338, Cell Signaling Technologies (CST), Beverly, MA, USA), phos-Smad3 (1:1000, #9520, CST), and GAPDH(1:5000, #ab8245, Abcam).

Statistical Analyses

All data were displayed as mean \pm standard deviation (SD) on the basis of 3 repetitions. Data analysis and graphing were based on SPSS PASW Statistics (version 17.0) and GraphPad Prism (version 5.0). For difference between any 2 groups, the data were compared using the paired *t*-test, while among multiple groups were tested by 1-way or 2-way analysis of variance (ANOVA) followed by Tukey's post hoc test. *p* value less than 0.05 was deemed as significant difference.

Table 2. Correlation Between DARS-AS1 Expression and Clinical Characteristics of AML Patients.

Clinicopathological Variables	High DARS-AS1 (n = 30)	Low DARS-AS1 (n = 29)	<i>p</i> value
Age (Years)	5.79 \pm 2.34	6.08 \pm 2.69	0.688
Gender (male/female)	16/14	15/14	> 0.999
White blood cells ($\times 10^9/L$)	17.26 \pm 9.41	10.48 \pm 5.27	0.003
Hemoglobin (g/L)	51.25 \pm 27.45	82.69 \pm 30.70	0.0004
Platelet count ($\times 10^9/L$)	35.18 \pm 25.77	56.93 \pm 31.86	0.011
FAB classification			0.89
M1/M2	13	11	
M4/M5	10	12	
M0/M6	7	6	

Note: AML, acute myeloid leukemia; DARS-AS1, aspartyl-tRNA synthetase anti-sense 1; FAB, French-American-British.

Results

DARS-AS1 Expresses Highly in AML Patients and Cells and Is Associated With Dismal Prognosis

We first analyzed DARS-AS1 expression in bone marrow from 34 healthy subjects and 59 AML patients. DARS-AS1 expression was much higher in bone marrow from AML patients than that in healthy subjects (Figure 1A). Moreover, we further analyzed the association between DARS-AS1 and 5-year survival rate of AML patients. Patients with highly expressed DARS-AS1 had lower 5-year survival than those with poorly expressed DARS-AS1 (Figure 1B). We found that the number of leukocytes in the peripheral blood of AML patients with high expression of DARS-AS1 was significantly higher, and the hemoglobin content and platelet count were significantly lower than that of patients with low expression of DARS-AS1. However, the expression of DARS-AS1 was not related to French-American-British classification, age and gender (Table 2).

Subsequently, the expression of DARS-AS1 in 4 AML cell lines BF-24, MV4-11, U937, HL-60 and HS-5 bone marrow stromal cells was measured. As shown in Figure 1C, DARS-AS1 expression was notably elevated in AML cells versus HS-5 cells.

Knockdown of DARS-AS1 Inhibits the Proliferation of AML Cells

The expression of DARS-AS1 was higher in MV4-11 and BF-24 cells relative to the other 2 AML cell lines, and 2 designed shRNAs targeting DARS-AS1 were transfected into MV4-11 and BF-24 cells, respectively. At 24-h post-transfection, RT-qPCR was carried out to verify the successful development of MV4-11 and BF-24 cells poorly-expressing DARS-AS1, and the intervention efficiency was the highest for shRDARS-AS1-#2 (Figure 2A). After knocking-down DARS-AS1, the number of cell colonies formed by MV4-11 and BF-24 cells was significantly reduced (Figure 2B), and the proliferation of cells was greatly weakened (Figure 2C). Moreover, under the action of shDARS-AS1, viability of MV4-AS1 and BF-24 cells was significantly inhibited, and the activity of Caspase-3 in cells was significantly increased (Figure 2D and E), indicating that apoptosis was promoted after DARS-AS1 knockdown. To verify the function of DARS-AS1 on apoptosis, we analyzed apoptosis by flow cytometry and observed that the proportion of apoptosis in MV4-AS1 and BF-24 cells was elevated by DARS-AS1 depletion (Figure 2F).

DARS-AS1 Depletion Inhibits the Growth of AML Cells In Vivo

To verify the function of DARS-AS1 on the growth of MV4-11 and BF-24 cells *in vivo*, we injected stably transfected MV4-11 and BF-24 cells into mice by subcutaneous injection. The tumor volume of mice injected with MV4-11 and BF-24 cells was measured every 3 days started at 5-day post-injection to assess the tumor growth rate *in vivo* (Figure 3A). After 35 days, the weight of tumors was significantly smaller than that of tumor induced by shScramble-transfected cells (Figure 3B). Then, we used immunohistochemistry to detect the rate of KI67-positive cells in tumor tissues. After DARS-AS1 down-regulation, the number of KI67-positive cells in tumors formed by MV4-11 and BF-24 cells was significantly reduced as well (Figure 3C).

DARS-AS1 Is Located in the Cytoplasm

To determine the downstream molecular mechanisms of the DARS-AS1, we first predicted subcellular localization of DARS-AS1 in various cells through LncAtlas website (<http://lncatlas.org.eu/>). DARS-AS1 was distributed either in cytoplasm or nucleus in different cells (Figure 4A). Therefore, we applied FISH assays to detect subcellular localization of DARS-AS1 in MV4-11 and BF-24 cells, and observed that the DARS-AS1 probe with red fluorescence mainly existed in cytoplasm (Figure 4B). Moreover, the nuclear/cytoplasmic

fractionation also demonstrated that DARS-AS1 was mainly present in cytoplasm (Figure 4C) relative to U6 or GAPDH in MV4-11 and BF-24 cells.

DARS-AS1 Promotes TGFBI Expression by Competitive Binding to miR-425

Subsequently, we predicted the binding relationship between miR-425 and DARS-AS1 through the bioinformatics website RNA22 (cm.jefferson.edu/rna22/). miR-425 was observed to share binding sites with DARS-AS1 (Figure 5A). Therefore, synthesized DARS-AS1 WT and MT luciferase reporter vectors based on this prediction were co-transfected with miR-425 mimic or mimic control into 293 T cells. The luciferase activity in cells transfected with miR-425 mimic and DARS-AS1 WT decreased significantly (Figure 5B). Furthermore, our RNA pull-down experiments using biotin-labeled miR-425 revealed that miR-425 can pull-down more DARS-AS1 (Figure 5C). Subsequently, we further analyzed miR-425 expression in the bone marrow of 34 healthy subjects and 59 AML patients. miR-425 was poorly expressed in AML patients (Figure 5D) and negatively correlated with DARS-AS1 expression in 59 patients (Figure 5E). Moreover, we detected miR-425 expression in MV4-11 and BF-24 cells with DARS-AS1 knockdown and found that after DARS-AS1 knockdown, the miR-425 expression was increased significantly (Figure 5F).

We further used TargetScan (<http://www.targetscan.org/>) website to predict possible targeting mRNAs, which revealed that TGFBI was a putative target of miR-425 (Figure 5G). We then tested the binding relationship between miR-425 and TGFBI using dual-luciferase reporter assays. The luciferase activity in the TGFBI WT group was notably decreased following introduction of miR-425 mimic (Figure 5H). Subsequently, we examined TGFBI expression in healthy subjects and AML patients. TGFBI expression was significantly higher in AML patients than that in healthy subjects (Figure 5I). TGFBI was positively correlated with DARS-AS1 expression (Figure 5J) and negatively correlated with miR-425 expression (Figure 5K). Moreover, we found a significant decline in mRNA and protein expression of TGFBI in MV4-11 and BF-24 cells with low expression of DARS-AS1 (Figure 5L and M).

miR-425 Inhibition or TGFBI Overexpression Abolishes the Inhibitory Role of shDARS-AS1 in AML Cells

To further validate the role of miR-425 and TGFBI in AML cells, we further transfected miR-425 inhibitor or oe-TGFBI into cells stably expressing shDARS-AS1. Successful transfection was validated using RT-qPCR and western blot (Figure 6A and B). After further knocking-down miR-425 expression or overexpressing TGFBI in AML cells poorly expressing DARS-AS1, the number of colonies formed by MV4-11 and BF-24 cells increased significantly, and the proliferative ability of cells was significantly enhanced (Figure 6C and D). Moreover, inhibition of miR-425 or

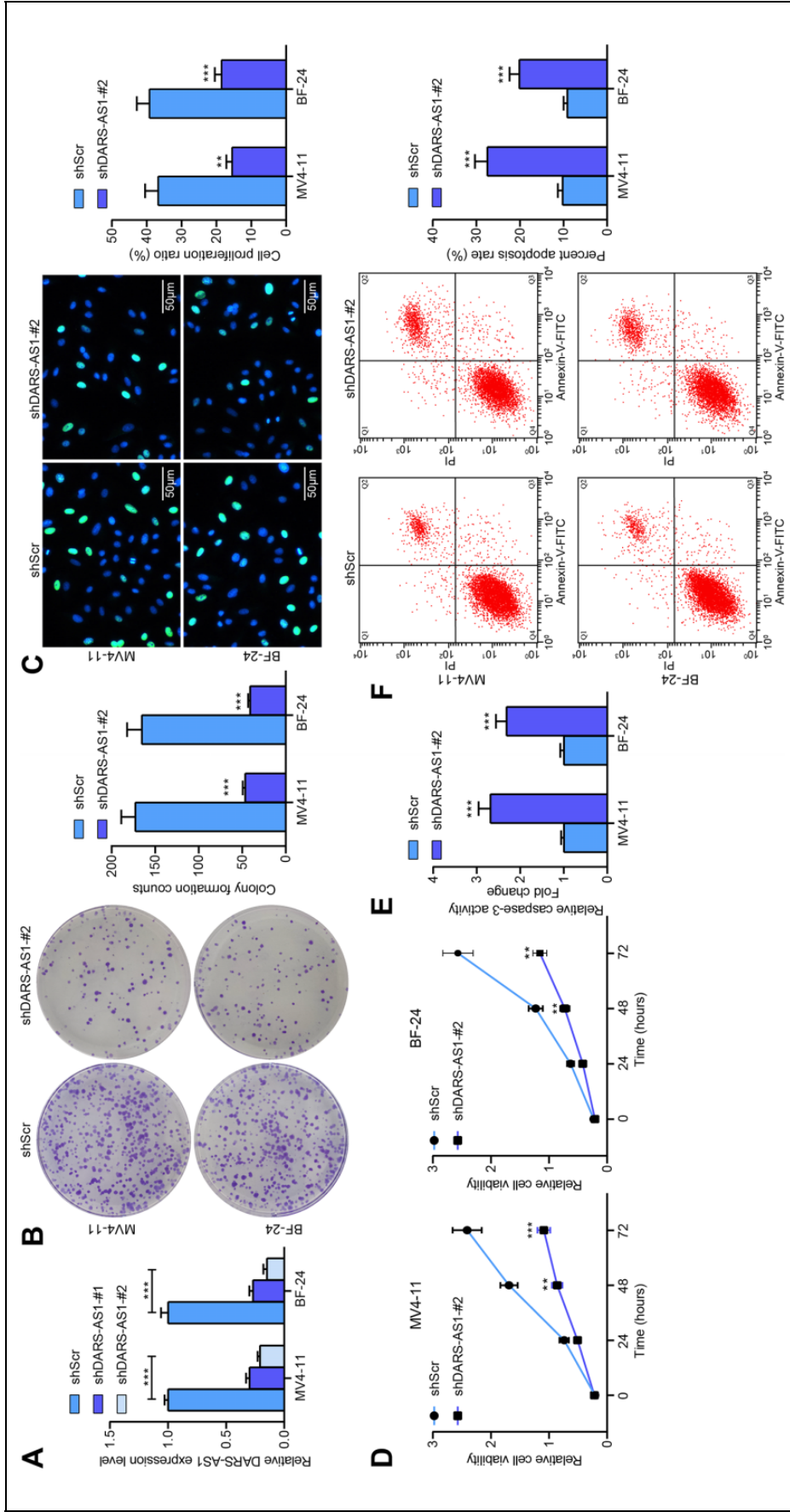


Figure 2. Knockdown of DARS-AS1 inhibits the growth of AML cells *in vitro*. Two shRNAs targeting DARS-AS1 were transfected into MV4-11 and BF-24 cells. A, RT-qPCR detection of DARS-AS1 expression in cells after transfection; B, the number of colonies formed by MV4-11 and BF-24 cells detected by colony formation assay; C, EdU staining for cell proliferation; D, MV4-11 and BF-24 cell viability after transfection with shDARS-AS1; E, Caspase-3 activity in MV4-11 and BF-24 cells detected by kits; F, the apoptosis ratio of MV4-11 and BF-24 cells detected by flow cytometry. Data were represented as mean \pm SD of 3 individual experiments. Two-way ANOVA followed by Tukey's post hoc test was utilized for data analysis among multiple groups. ** $p < 0.01$; *** $p < 0.001$.

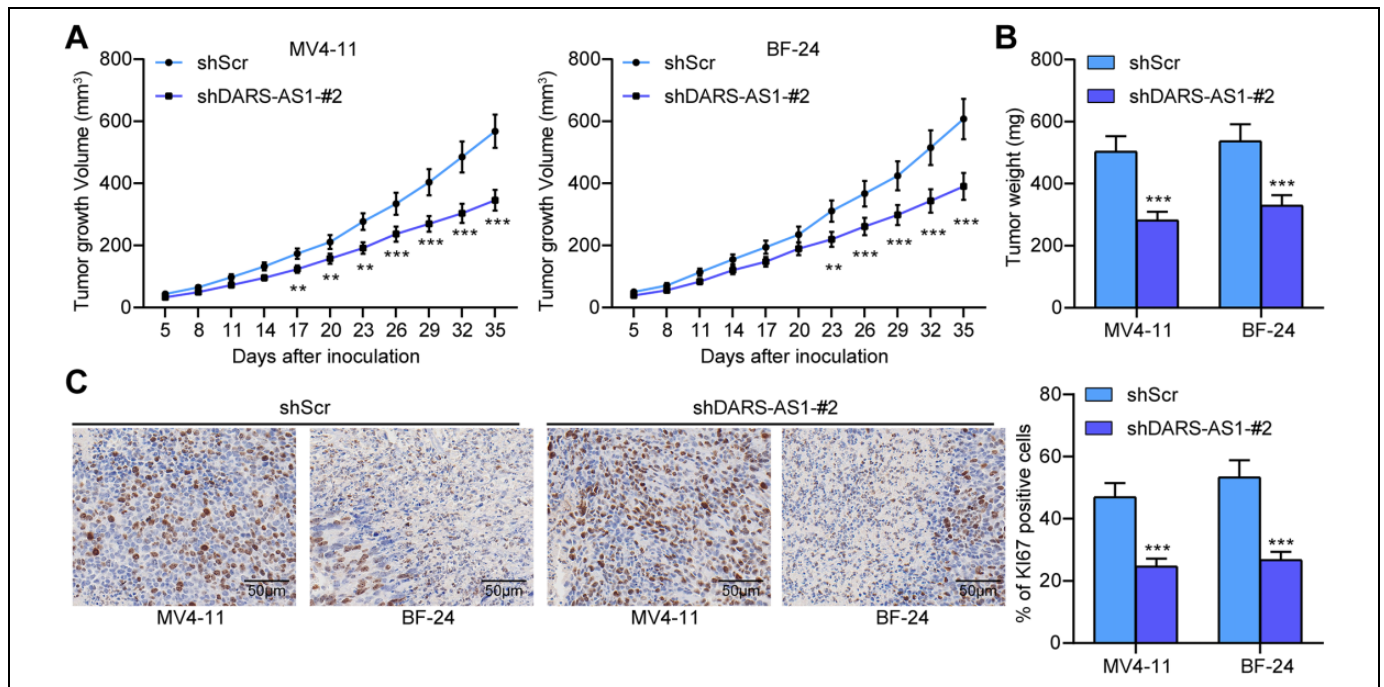


Figure 3. Knockdown of DARS-AS1 inhibits AML cell growth *in vivo*. MV4-11 and BF-24 cells expressing shDARS-AS1 were subcutaneously injected into mice (n = 5). A, tumor volumes of nude mice were measured every 3 days beginning at 5-day post-injection; B, weight of tumors formed by MV4-11 and BF-24 cells; C, the number of Ki67-positive cells in MV4-11 and BF-24 cell-forming xenograft tumors was detected by immunohistochemistry. Data were represented as mean ± SD of 3 individual experiments. Two-way ANOVA followed by Tukey’s post hoc test was applied for data analysis among multiple groups. ** $p < 0.01$; *** $p < 0.001$.

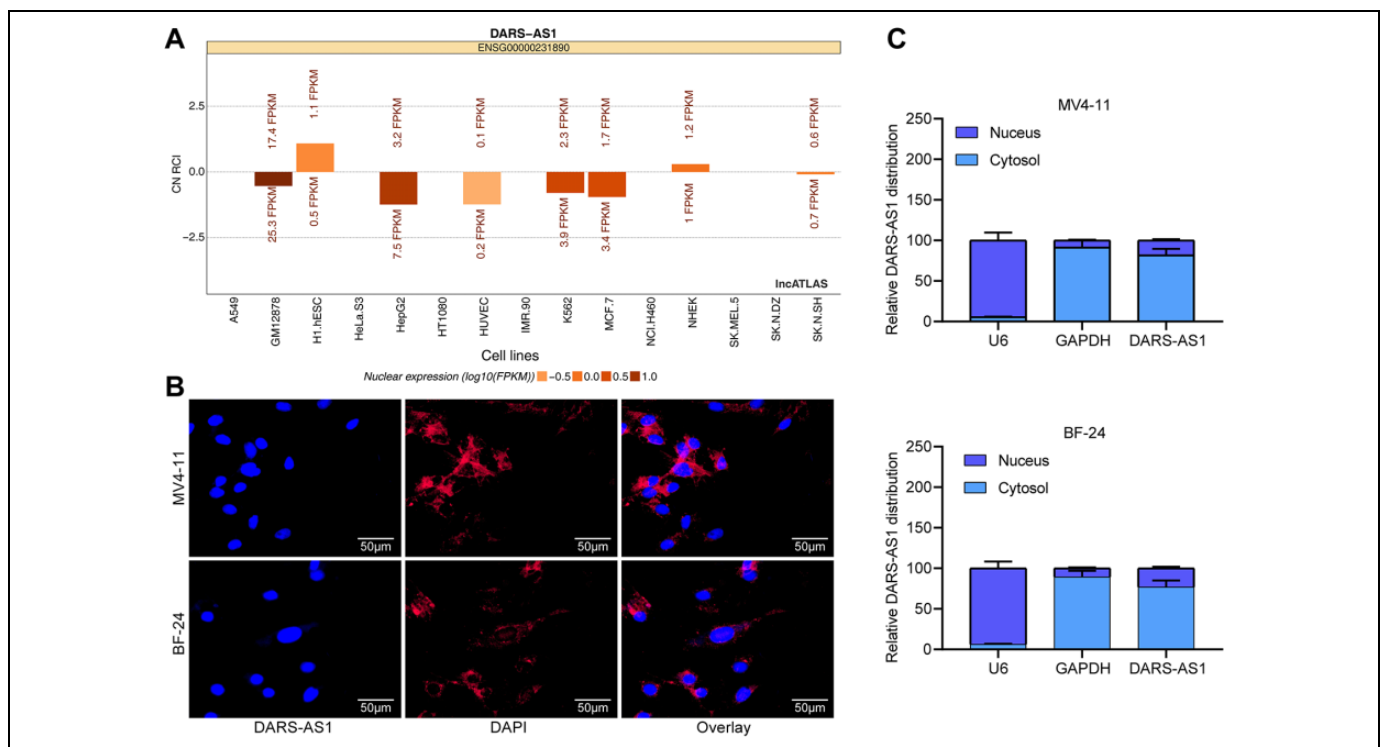


Figure 4. DARS-AS1 is localized in the cytoplasm. A, subcellular localization of DARS-AS1 in various cells predicted by LncAtlas (<http://lncatlas.crg.eu/>); B, FISH assay detection of subcellular localization of DARS-AS1 in MV4-11 and BF-24 cells where red fluorescence represented DARS-AS1 probe and blue represented nucleus; C, the subcellular localization of DARS-AS1 in MV4-11 and BF-24 cells detected by nuclear/cytoplasmic fractionation with U6 as control of nucleus and GAPDH as control of cytoplasm.

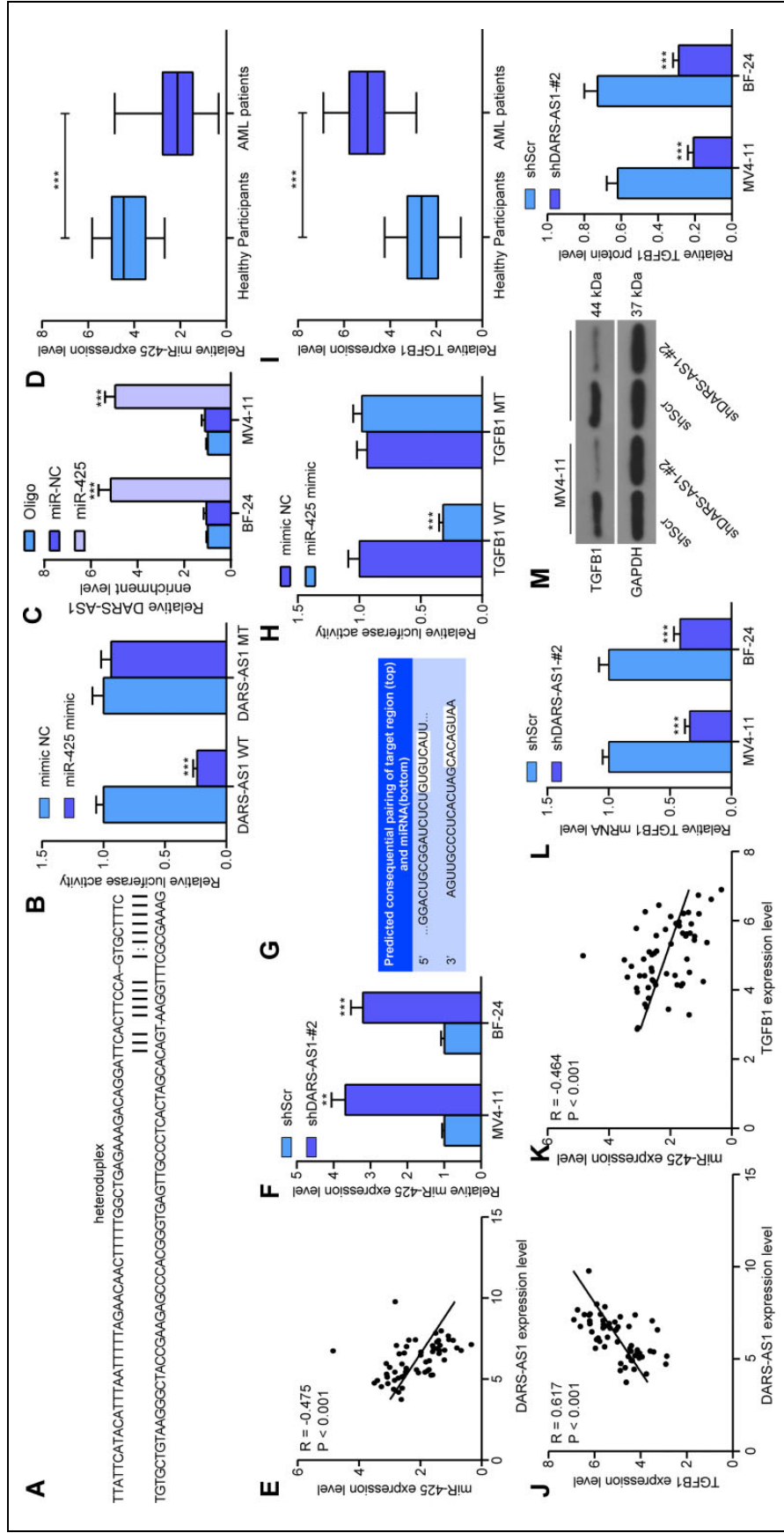


Figure 5. DARS-AS1 promotes TGFB1 expression by competitive binding to miR-425. **A**, RNA22 bioinformatics website prediction of miR-425 and DARS-AS1 binding sites; **B**, dual-luciferase validation of binding relationship between miR-425 and DARS-AS1 in 293 T cells; **C**, the binding of miR-425 to DARS-AS1 assessed by biotin-labeled RNA pull-down assay; **D**, RT-qPCR detection of miR-425 expression in the bone marrow of 34 healthy subjects and 59 AML patients; **E**, Pearson correlation analysis of the correlation between DARS-AS1 and miR-425 in 59 patients; **F**, RT-qPCR detection of miR-425 expression in MV4-11 and BF-24 cells stably expressing shDARS-AS1; **G**, TargetScan (<http://www.targetscan.org/>) website prediction of possible targeting mRNA of miR-425; **H**, dual-luciferase validation of binding relationship between miR-425 and TGFB1 in 293 T cells; **I**, RT-qPCR detection of TGFB1 expression in the bone marrow of 34 healthy subjects and 59 AML patients; **J**, Pearson correlation analysis of the correlation between DARS-AS1 and TGFB1 expression in 59 patients; **K**, Pearson correlation analysis of the correlation between miR-425 and TGFB1 expression in 59 patients; **L**, RT-qPCR detection of TGFB1 mRNA expression in MV4-11 and BF-24 cells stably expressing shDARS-AS1; **M**, western blot analysis of TGFB1 protein expression in MV4-11 and BF-24 cells stably expressing shDARS-AS1. Data were represented as mean \pm SD of 3 individual experiments. Each dot in the panel E, J and K represents a subject. The data between 2 groups were analyzed using paired *t*-test (panel D and I), and 2-way ANOVA followed by Tukey's post hoc test was applied for data analysis among multiple groups (panel B, C, F, H, L and M). ** $p < 0.01$, *** $p < 0.001$.

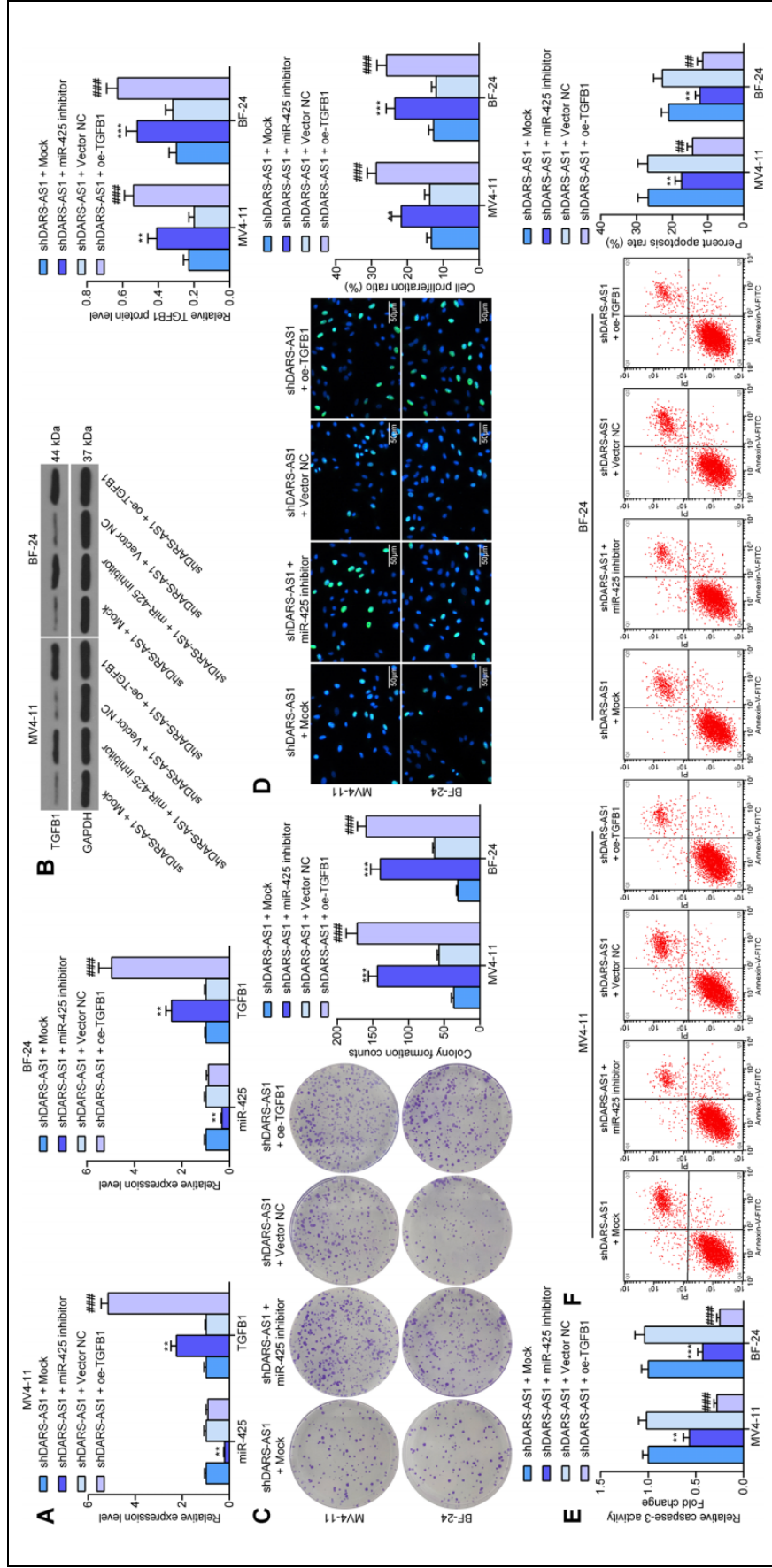


Figure 6. miR-425 inhibitor or overexpression of TGFB1 abolishes the inhibitory role of shDARS-AS1 in AML cells. miR-425 inhibitor and oe-TGFB1 were further transfected into MV4-11 and BF-24 cells with stable knockdown of DARS-AS1. A, RT-qPCR detection of miR-425 and TGFB1 mRNA expression in MV4-11 and BF-24 cells after co-transfection; B, western blot analysis of TGFB1 protein expression in MV4-11 and BF-24 cells after co-transfection; C, the number of colonies formed by MV4-11 and BF-24 cells detected by colony formation assay; D, MV4-11 and BF-24 cell viability after co-transfection; E, Caspase-3 activity in MV4-11 and BF-24 cells detected by kits; F, the apoptosis ratio of MV4-11 and BF-24 cells detected by flow cytometry. Data were represented as mean \pm SD of 3 individual experiments. Two-way ANOVA followed by Tukey's test was applied for data analysis among multiple groups. ** $p < 0.01$; *** $p < 0.001$ vs. cells transfected with shDARS-AS1 + Mock; ## $p < 0.01$; ### $p < 0.001$ vs. cells transfected with shDARS-AS1 + Vector NC.

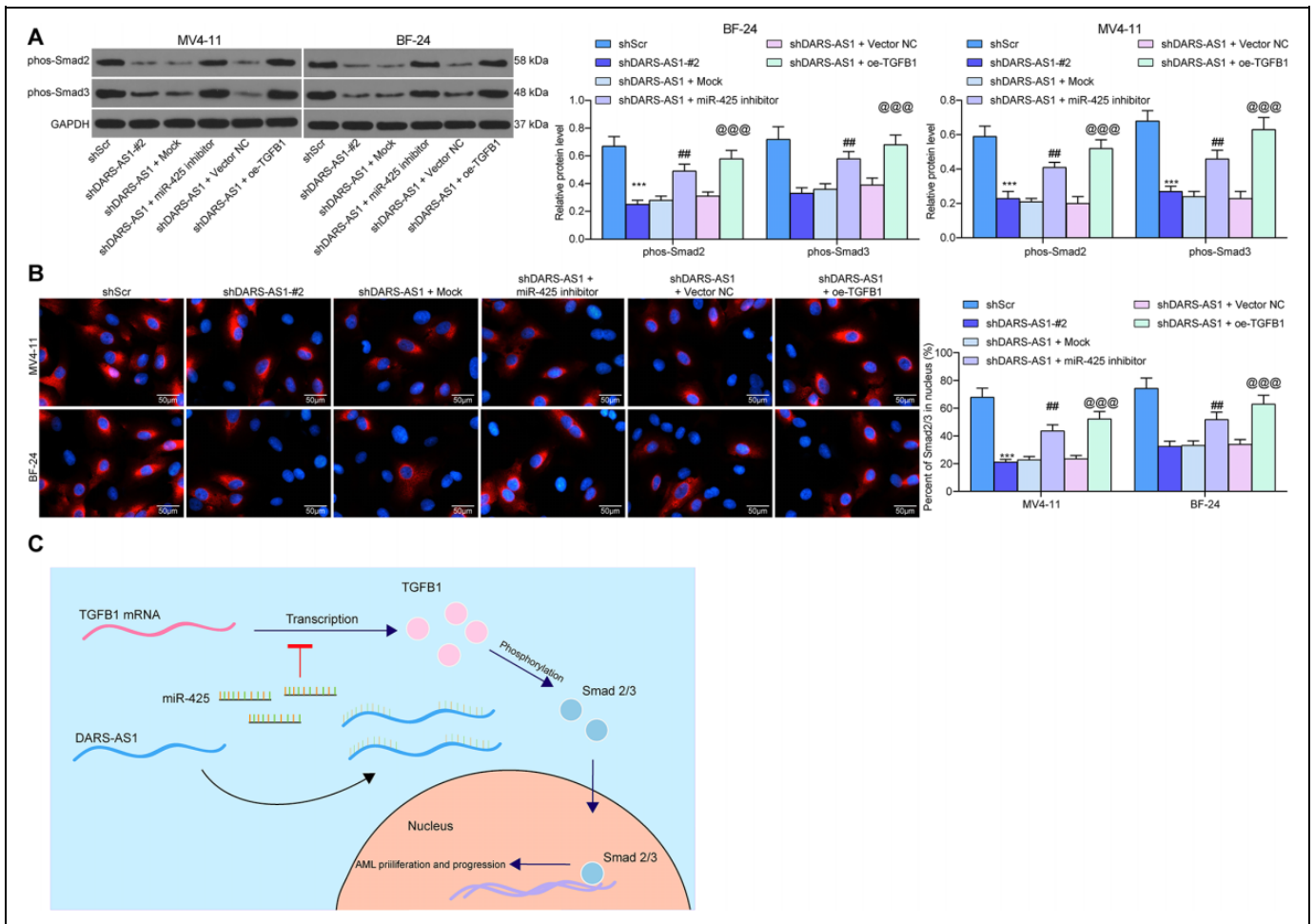


Figure 7. TGFβ1 promoted Smad2/3 phosphorylation and nuclear translocation. A, western blot analysis of Smad2/3 phosphorylation levels in MV4-11 and BF-24 cells; B, immunofluorescence staining identification of Smad2/3 subcellular localization; C, schematic representation of DARS-AS1 regulation of the miR-425/TGFβ1/Smad2/3 axis and its impact on cancerous progression in AML cells. Data were represented as mean \pm SD of 3 individual experiments. Two-way ANOVA followed by Tukey's test was applied for data analysis among multiple groups. *** $p < 0.001$ vs. cells transfected with shScr; ## $p < 0.01$ vs. cells transfected with shDARS-AS1 + Mock; @@@ $p < 0.001$ vs. cells transfected with shDARS-AS1 + Vector NC.

overexpression of TGFβ1 in the presence of shDARS-AS1 led to significantly inhibited Caspase-3 activity and decreased apoptotic proportion (Figure 6E and F).

TGFβ1 Promotes Smad2/3 Phosphorylation and Nuclear Translocation

Western blot assays were first used to detect the extent of Smad2/3 phosphorylation in MV4-11 and BF-24 cells. After DARS-AS1 knockdown, the extent of Smad2/3 phosphorylation was remarkably inhibited, however, further miR-425 inhibition or TGFβ1 overexpression increased the extent of Smad2/3 phosphorylation (Figure 7A). After phosphorylation of Smad2 and Smad3, they function as transcription factors to regulate the transcription of downstream genes, thus promoting cell growth. Thus, we used immunofluorescence to detect subcellular localization of Smad2/3 in MV4-11 and BF-24 cells. Decreased expression of DARS-AS1 in cells

significantly inhibited Smad2/3 nuclear translocation, while further reduced miR-425 or increased TGFβ1 expression in cells promoted Smad2/3 nuclear translocation (Figure 7B). Overall, DARS-AS1 promoted TGFβ1 expression through competitively binding to miR-425, thereby inducing Smad2/3 phosphorylation and nuclear translocation to promote AML cell growth (Figure 7C).

Discussion

Due to the application of microarrays analysis and high-throughput sequencing in whole genomes and transcriptomes, it is now well-established that less than 2% of the genome encodes proteins, and at least 75% is transcribed into noncoding RNAs, among which those surpass 200 nucleotides in length were termed as lncRNAs.¹⁴ Several mechanisms have been established to elucidate the role of lncRNAs in tumorigenesis, involving mRNA and protein stability regulation,

transcriptional and translational modulation as well as competing endogenous RNA mechanism.¹⁵ Multiple lncRNAs, involving NEAT1, UCA1 and SNHG5 have been reported to participate in the progression of AML through regulating miRNA/mRNA networks.¹⁶⁻¹⁸ In this report, DARS-AS1 was observed to be upregulated in the bone marrow tissues of AML pediatric patients and AML cells, and its expression pattern was conversely correlated with the 5-year survival of patients with AML. Furthermore, knockdown of DARS-AS1 repressed the proliferation of AML cells both *in vitro* and *in vivo*, and facilitated the apoptosis of AML cells. Additionally, our findings illuminated that DARS-AS1 positively regulated the TGF β 1 expression through binding to miR-425 to modulate the Smad2/3 pathway of AML cells.

It has been shown that DARS-AS1 was notably promoted in thyroid cancer tissues relative to matched adjacent tissues, and was positively linked to tumor stage, distant metastasis and dismal prognosis of patients.¹⁹ Furthermore, hypoxia-induced DARS-AS1 enhanced myeloma malignancy by mediating the stability of RNA-binding motif protein 39.²⁰ In the current work, DARS-AS1 was observed to be highly expressed in AML cells (BF-24, MV4-11, U937, HL-60) relative to HS-5 cells and as expected, DARS-AS1 depletion hampered proliferation and stimulated apoptosis in both MV4-11 and BF-24 cells. Furthermore, we demonstrated that DARS-AS1 knockdown suppressed MV4-11 and BF-24 cell tumorigenesis *in vivo*. These findings fill the knowledge gap of the cancer-initiating function of DARS-AS1 in AML, emphasizing DARS-AS1 as an attracting therapeutic option for AML. Subsequently, DARS-AS1 was substantiated to mainly distribute in AML cell cytoplasm, which inspired us to analyze the post-transcriptional regulatory mechanism of DARS-AS1 in AML cells. The proposed mechanism for the oncogenic role of DARS-AS1 in AML is its capacity of sponging certain miRNAs. With the help of bioinformatics analyses, dual-luciferase reporter as well as RNA pull-down assays, miR-425 was identified as a possible downstream miRNA of DARS-AS1 and to share a binding relationship with it. Importantly, the anti-proliferative and pro-apoptotic effects of DARS-AS1 knockdown was overturned by miR-425 inhibitor, implying that DARS-AS1 contributes to AML progression by sponging miR-425. miR-425 has been demonstrated to exert tumor-suppressing effects in glioma by acting as a lncRNA sponge.²¹ In addition, miR-425 upregulation has been recently proposed to indicate better prognosis in younger AML patients receiving chemotherapy.²²

In the present study, we also identified TGF β 1 as a target of miR-425. Induced TGF β 1 transcription by liver-specific bHLH-Zip transcription factor was involved in the potentiated triple-negative breast cancer progression.²³ Under the context of AML, TGF β was upregulated in hematopoietic stem cells from bone marrow of AML mice because of excessive production of TGF β 1 from megakaryocytes and overactivation of latent TGF β 1 protein.²⁴ Also, it has been suggested that TGF- β 1 expression was enriched in different human AML cells, including OCI-AML1, AML193 and THP-1 cells, and

the proliferation and differentiation of the AML cells are regulated by TGF- β 1 via autocrine and paracrine pathways.²⁵ In line with our data, TGF- β 1 significantly promoted cell proliferation, yet suppressed caspase-3 activity and cell apoptosis in MG-63 cells.²⁶ In cervical cancer, TGF- β 1 abolished the effects of C glycoprotein on the declines in cell migration and promotion of apoptosis,²⁷ which is largely in agreement with the observations of our study that TGF- β 1 overexpression reversed the suppressive role of shDARS-AS1 in cell proliferation and promotive role in cell apoptosis. Moreover, Smad2 and Smad3, grouped together as TGF- β -specific R-Smads,²⁸ have been observed to be phosphorylated and underwent nuclear translocation following TGF β 1. Jung et al has also documented that poor TGF β 1 mRNA expression was expected to attenuate the TGF- β /Smad cascade.²⁹ Interestingly, miR-425 expedite granulosa cells apoptosis by targeting TGFBR2, a TGF- β receptor, and the following canonical TGF- β pathway, which was rescued by Smad4 and TGF- β 1.³⁰ The similar associations between TGF β 1 and miR-425 or Smad were notable in the current investigation as well.

Conclusion

All in all, the results in the present study illustrate that DARS-AS1 knockdown curtails cell proliferation and drives apoptosis by regulating miR-425/TGF β 1/Smad2/3 axis in AML. Our findings might provide the feasibility for applying lncRNA-based therapies in AML treatment.

Authors' Note

The study was authorized by the Ethics Committee of the First Affiliated Hospital of Zhengzhou University (approval no. 201304011) with the permission of all participants and their guardians by providing informed consent.

Declaration of Conflicting Interests

The author(s) declared no potential conflicts of interest with respect to the research, authorship, and/or publication of this article.

Funding

The author(s) received no financial support for the research, authorship, and/or publication of this article.

ORCID iD

Guangyao Sheng  <https://orcid.org/0000-0002-1756-5257>

References

1. Burnett A, Wetzler M, Lowenberg B. Therapeutic advances in acute myeloid leukemia. *J Clin Oncol.* 2011;29(5):487-494.
2. Dohner H, Weisdorf DJ, Bloomfield CD. Acute myeloid leukemia. *N Engl J Med.* 2015;373(12):1136-1152.
3. Rubnitz JE. Current management of childhood acute myeloid leukemia. *Paediatr Drugs.* 2017;19(1):1-10.
4. Zimta AA, Tomuleasa C, Sahnoune I, Calin GA, Berindan-Neagoe I. Long non-coding RNAs in myeloid malignancies. *Front Oncol.* 2019;9:1048.

5. Gourvest M, Brousset P, Bousquet M. Long noncoding RNAs in acute myeloid leukemia: functional characterization and clinical relevance. *Cancers (Basel)*. 2019;11(11):1638.
6. Huang K, Fan WS, Fu XY, Li YL, Meng YG. Long noncoding RNA DARS-AS1 acts as an oncogene by targeting miR-532-3p in ovarian cancer. *Eur Rev Med Pharmacol Sci*. 2019;23(6):2353-2359.
7. Liu D, Liu H, Jiang Z, Chen M, Gao S. Long non-coding RNA DARS-AS1 promotes tumorigenesis of non-small cell lung cancer via targeting miR-532-3p. *Minerva Med*. 2019. doi:10.23736/S0026-4806.19.06198-6.
8. Chen L, Wang W, Cao L, Li Z, Wang X. Long non-coding RNA CCAT1 acts as a competing endogenous RNA to regulate cell growth and differentiation in acute myeloid leukemia. *Mol Cells*. 2016;39(4):330-336.
9. Jiao M, Guo H, Chen Y, Li L, Zhang L. DARS-AS1 promotes clear cell renal cell carcinoma by sequestering miR-194-5p to up-regulate DARS. *Biomed Pharmacother*. 2020;128:110323.
10. Xiao H, Liang S, Wang L. Competing endogenous RNA regulation in hematologic malignancies. *Clin Chim Acta*. 2020;509:108-116.
11. Liu P, Hu Y, Ma L, Du M, Xia L, Hu Z. miR-425 inhibits melanoma metastasis through repression of PI3K-Akt pathway by targeting IGF-1. *Biomed Pharmacother*. 2015;75:51-57.
12. Yao X, Liu C, Liu C, Xi W, Sun S, Gao Z. lncRNA SNHG7 sponges miR-425 to promote proliferation, migration, and invasion of hepatic carcinoma cells via Wnt/beta-catenin/EMT signaling pathway. *Cell Biochem Funct*. 2019;37(7):525-533.
13. Gu S, Feng XH. TGF-beta signaling in cancer. *Acta Biochim Biophys Sin (Shanghai)*. 2018;50(10):941-949.
14. Huarte M. The emerging role of lncRNAs in cancer. *Nat Med*. 2015;21(11):1253-1261.
15. Zhang XZ, Liu H, Chen SR. Mechanisms of long non-coding RNAs in cancers and their dynamic regulations. *Cancers (Basel)*. 2020;12(5):1245.
16. Feng S, Liu N, Chen X, Liu Y, An J. Long non-coding RNA NEAT1/miR-338-3p axis impedes the progression of acute myeloid leukemia via regulating CREBRF. *Cancer Cell Int*. 2020;20:112.
17. Li J, Wang M, Chen X. Long non-coding RNA UCA1 modulates cell proliferation and apoptosis by regulating miR-296-3p/Myc axis in acute myeloid leukemia. *Cell Cycle*. 2020;19(12):1454-1465.
18. Ying X, Zhang W, Fang M, Wang C, Han L, Yang C. LncRNA SNHG5 regulates SOX4 expression through competitive binding to miR-489-3p in acute myeloid leukemia. *Inflamm Res*. 2020;69(6):607-618.
19. Zheng W, Tian X, Cai L, et al. LncRNA DARS-AS1 regulates microRNA-129 to promote malignant progression of thyroid cancer. *Eur Rev Med Pharmacol Sci*. 2019;23(23):10443-10452.
20. Tong J, Xu X, Zhang Z, et al. Hypoxia-induced long non-coding RNA DARS-AS1 regulates RBM39 stability to promote myeloma malignancy. *Haematologica*. 2020;105(6):1630-1640.
21. Cao S, Zheng J, Liu X, et al. FXR1 promotes the malignant biological behavior of glioma cells via stabilizing MIR17HG. *J Exp Clin Cancer Res*. 2019;38(1):37.
22. Zhang J, Shi J, Zhang G, et al. MicroRNA-425 upregulation indicates better prognosis in younger acute myeloid leukemia patients undergoing chemotherapy. *Oncol Lett*. 2019;17(6):5793-5802.
23. Tang X, Zhou Y, Liu Y, Zhang W, Liu C, Yan C. Potentiation of cancerous progression by LISCH7 via direct stimulation of TGFBI transcription in triple-negative breast cancer. *J Cell Biochem*. 2020.
24. Gong Y, Zhao M, Yang W, et al. Megakaryocyte-derived excessive transforming growth factor beta1 inhibits proliferation of normal hematopoietic stem cells in acute myeloid leukemia. *Exp Hematol*. 2018;60:40-46. e42.
25. Ma W, Qin Y, Chapuy B, Lu C. LRRC33 is a novel binding and potential regulating protein of TGF-beta1 function in human acute myeloid leukemia cells. *PLoS One*. 2019;14(10):e0213482.
26. Wang WD, Cheng BZ, Kang WB, Zheng RW, Cai YL, Wang XJ. Investigation for TGF-beta1 expression in type 2 diabetes and protective effects of TGF-beta1 on osteoblasts under high glucose environment. *Eur Rev Med Pharmacol Sci*. 2018;22(19):6500-6506.
27. Wang DG, Li TM, Liu X. RHCG suppresses cervical cancer progression through inhibiting migration and inducing apoptosis regulated by TGF-beta1. *Biochem Biophys Res Commun*. 2018;503(1):86-93.
28. Matsuzaki K. Smad phosphoisoform signaling specificity: the right place at the right time. *Carcinogenesis*. 2011;32(11):1578-1588.
29. Jung M, Lee JH, Lee C, Park JH, Park YR, Moon KC. Prognostic implication of pAMPK immunohistochemical staining by subcellular location and its association with SMAD protein expression in clear cell renal cell carcinoma. *Cancers (Basel)*. 2019;11(10):1602.
30. Du X, Pan Z, Li Q, Liu H, Li Q. SMAD4 feedback regulates the canonical TGF-beta signaling pathway to control granulosa cell apoptosis. *Cell Death Dis*. 2018;9(2):151.